Specular reflections of transient pressures from finite width plane faces

C. S. Clay
Department of Geology and Geophysics, Weeks Hall, University of Wisconsin, Madison, Wisconsin 53706

Dezhang Chu
Department of Applied Ocean Physics and Engineering Woods Hole Oceanographic Institution, Woods Hole, Massachusetts 02543

Saimu Li
Ocean University of Qing Dao, Qing Dao, Shandon& People's Republic of China
(Received 9 June 1992; accepted for publication 21 June 1993)

The reflections of transient pressure signals from hard (perfectly reflecting) finite width plane facets have been studied theoretically and experimentally. The experiments and theory used point sources, and sound pressures were observed in the specular direction. Theoretical solutions used the Helmholtz-Kirchhoff integral and incident spherical waves in the Fresnel approximation. The results of these laboratory experiments are compared to numerical evaluations of the integrals. Applications to acoustical oceanography and to architectural acoustics are: the specular reflection of waves from a reflecting facet on the seafloor and the specular reflection of sound waves from sound deflectors above a performer on a stage.
PACS numbers: 43.30.Gv, 43.20.Fn, 43.20.Bi, 43.SS.Fw

INTRODUCTION

Most computations of waves scattered and reflected at rough interfaces use either the incident spherical waves (usually in the Fresnel approximation) or the incident plane-wave approximation (Fraunhofer). The reflection and scattering of waves by a finite-dimensioned plane facet gives the problem in its elemental form. We will study the transition from the Fraunhofer region, where the dimensions of a facet are less than the first Fresnel zone, to the Fresnel region where the facets are larger than the first Fresnel zone. Neubauer and Dragonette made a set of laboratory measurements of the reflections of effectively continuous wave pressures from blocks of various "hard" materials in water.l They got excellent agreement between the measurements and evaluations of the HelmholtzKirchhoff integral.

As an extension of the usual solutions for harmonic waves, we calculate the amplitudes of transient pressures reflected from finite width plane facets. Figure 1 shows various sizes of facets superimposed on the Fresnel zones. As a simple approximation, there are two regions for facet reflection amplitudes. In Fig. 1(a) and (c), both dimensions of the facets are larger than the first Fresnel zone and we expect the wave to reflect with full amplitude. Then, the dimensions of the facet are effectively infinite. In the second region, Fig. 1(b) and (d), one facet dimension is less than the width of the first Fresnel zone and reflection amplitudes are reduced.

Clearly the reflection and diffraction of waves at finite width strips of facets are coupled, and reflected components from the Helmholtz-Kirchhoff integral are only part of the solution. Tolstoy published a pair of papers that give solutions for the diffractions by a hard (perfectly reflecting) truncated wedge, strip, and sound barriers[2,3]. However, he was primarily interested in the multiple diffraction part of the solution. In the wedge assembly or facet ensemble methods for calculating waves diffracted and reflected at rough seafloors and sea surfaces, one has both diffracted and reflected components. Diffracted components come from the intersections of the plane facets, i.e., wedge crests and troughs. Specularly reflected components come from the facets. We deal with the specularly reflected components in this paler. Computations of the diffraction components are in Refs. 8-14.

We mention applications of our results to architectural acoustics, concert halls, and the design of "acoustical adjustments." Many halls have acoustic devices over the stage that are intended to reflect and scatter sound into the audience. These devices are known as "reflectors," "clouds," and "deflectors." To be effective, the reflecting devices must reflect sound over a wide range of frequencies. The wavelengths of lowest frequencies, the distance of the reflecting devices above the performers, and spherical wave theory control the minimum dimensions of the reflectors.

I. AMPLITUDES OF REFLECTIONS FROM A PLANE FACET

We use the Helmholtz-Kirchhoff integral to make quantitative computations of the effects

of facet widths on reflection amplitudes. Since the Helmholtz-Kirchhoff integral is for continuous waves, we suppress the time dependence and calculate the pressure *P(f)* as a function of frequency f. Expressions for the Helmholtz-Kirchhoff integral are in Neubauer and Dragonette,1 Clay and Medwin (1977),15 and Clay (1990).14 Expressions from Clay and Medwin are designated as GM. After making the Kirchhoff approximation, the Helmholtz-Kirchhofl' integral is (C-M A10.5.7)

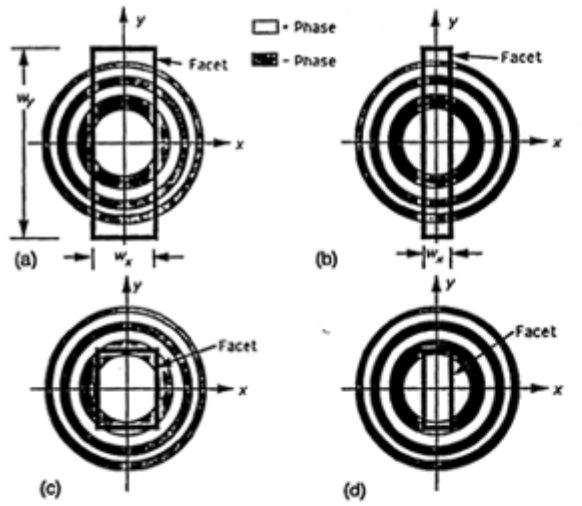

FIG. 1. Facets and the phases of the Fresnel zones, vertical incidence. The facet dimensions were chosen to cover all or a fraction of the first Fresnel zone. The facet width is w. Phases of the zones alternate: (a) Facet covers the first Fresnel zone in the x direction and several in the y direction. (b) Facet covers part of first Fresnel zone in the x direction and several in the y direction. (c) Facet covers the first Fresnel zone in the x direction and y direction. (d) Facet covers part of the first Fresnel zone in the x direction and the first zone in the y direction.

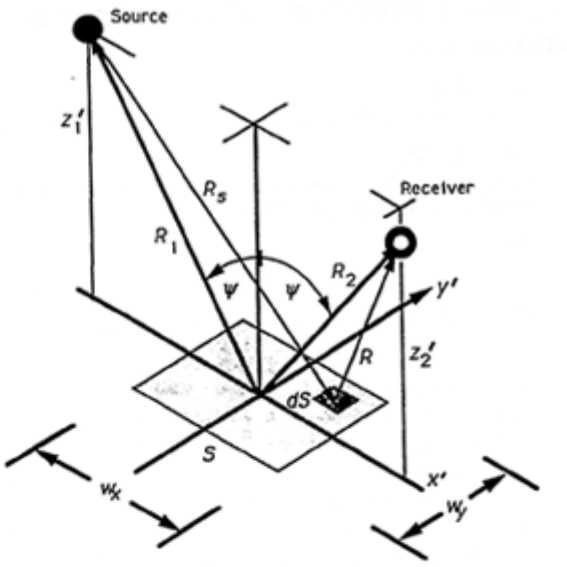

FIG. 2. Geometry for a Helmholtz–Kirchhoff–Fresnel calculation: The receiver is in the specular direction from the origin of the x'–y' coordinates of the surface S. The area dS is elevated $-\zeta$ above the surface S and at the coordinates x, y, and $-z$. The source and receiver are at different distances above the surface S. The facet dimensions w_x and w_y are shown.

Medwin are designated as C-M. After making the Kirchhoff approximation, the Helmholtz–Kirchhoff integral is (C-M A10.5.7)

$$P(f)\approx\frac{B\mathscr{R}_{12}}{4\pi}\int_s\frac{\partial}{\partial n}\left(\frac{\exp[-ik(R+R_s)]}{RR_s}\right)dS, \quad (1)$$

where k is the wave number $2\pi f/c$, B is a constant having the dimensions of pressure, the source directivity is unity, and the reflection coefficient is $\mathscr{R}_{12}$. The separations R and R_s are defined in Fig. 2. The x and y coordinates are on the surface of the facet. In the specular direction, the second-order approximation of $k(R+R_s)$ gives [use C-M Eq. (A10.5.7)–(A10.5.13) and change θ to ψ]

$$\psi_1=\psi_2=\psi, \quad (2)$$

$$k(R+R_s)\approx k(R_1+R_2)+x_f^{-2}x'^2+y_f^{-2}y'^2-2k\zeta\cos\psi, \quad (3)$$

$$x_f^{-2}\equiv\frac{k\cos^2\psi}{2}\left(\frac{R_1+R_2}{R_1R_2}\right), \quad (4)$$

$$y_f^{-2}\equiv\frac{k}{2}\left(\frac{R_1+R_2}{R_1R_2}\right), \quad (5)$$

where $-\zeta$ is the elevation of the area dS above the reference plane. The replacement of $k(R+R_s)$ by the second-order expansion of x' and y' in (3) is known as the Fresnel approximation. The normal derivative is

$$\frac{\partial}{\partial n}=\frac{\partial}{\partial\zeta}. \quad (6)$$

We make more simplifying approximations. Since the factor (RR_s) varies slowly, it can be replaced by (R_1R_2) and moved out of the integral. After the normal derivative is taken, ζ becomes 0 on the facet. The dependence of $\exp[-ik(R+R_s)]$ on x' and y' is important and this term stays in the integral. With these approximations, the integral (1) becomes

$$P(f)\approx\frac{iB\mathscr{R}_{12}k\cos\psi e^{-ik(R_1+R_2)}}{2\pi R_1R_2}\int_{-x_1}^{x_1}dx' \times\int_{-y_1}^{y_1}\exp\left(-i\frac{x'^2}{x_f^2}-i\frac{y'^2}{y_f^2}\right)dy', \quad (7)$$

where the limits x_1 and y_1 are the half-width and half-length of the facet. The expression contains the product of Fresnel integrals. The following changes of variables give the standard definitions of the Fresnel integrals, Abramowitz and Stegun (1965),[16] Sec. 7.3:

$$\frac{\pi}{2}u^2\equiv\frac{x'^2}{x_f^2}\text{ and }\frac{\pi}{2}v^2\equiv\frac{y'^2}{y_f^2}, \quad (8)$$

and the limits are

$$\frac{\pi}{2}u_1^2\equiv\frac{x_1'^2}{x_f^2}\text{ and }\frac{\pi}{2}v_1^2\equiv\frac{y_1'^2}{y_f^2}, \quad (9)$$

$$dS=dx'\,dy'=\frac{\pi}{2}x_fy_f\,du\,dv=\frac{\pi R_1R_2}{k\cos\psi(R_1+R_2)}. \quad (10)$$

The pressure becomes

$$P(f)\approx\frac{iB\mathscr{R}_{12}e^{-ik(R_1+R_2)}}{2(R_1+R_2)}I(u_1)I(v_1), \quad (11)$$

$$I(u_1)\equiv\int_{-u_1}^{u_1}\exp\left(-i\frac{\pi}{2}u^2\right)du$$

and (12)

$$I(v_1)\equiv\int_{-v_1}^{v_1}\exp\left(-i\frac{\pi}{2}v^2\right)dv,$$

and the cosine and sine integrals are

$$C(u_1)\equiv\int_0^{u_1}\cos\left(\frac{\pi}{2}u^2\right)du$$

and (13)

$$S(u_1)\equiv\int_0^{u_1}\sin\left(\frac{\pi}{2}u^2\right)du,$$

and

$$I(u_1)\equiv\int_{-u_1}^{u_1}\exp\left(-i\frac{\pi}{2}u^2\right)du=2[C(u_1)-iS(u_1)]. \quad (14)$$

The full facet dimensions are w_x and w_y and, correspondingly, the symmetric limits in the integrals are

$$x_1=w_x/2 \text{ and } y_1=w_y/2. \quad (15)$$

Using the definitions of u and v in (9), u_1 and v_1 are

$$u_1=\cos\psi\left(\frac{(R_1+R_2)}{2\lambda R_1R_2}\right)^{1/2}w_x, \quad (16)$$

$$v_1=\left(\frac{(R_1+R_2)}{2\lambda R_1R_2}\right)^{1/2}w_y, \quad (17)$$

where $\lambda=c/f$, c is sound velocity, and λ is wavelength.

A. Reflection from an infinite plane

The reflection from an infinite plane interface gives a reference pressure. The calculation also shows that the evaluation of the Helmholtz–Kirchhoff integral with the Fresnel approximation gives the familiar "image solution." Evaluations for infinite limits for the facet dimensions are

$$C(\infty)=0.5 \text{ and } S(\infty)=0.5, \quad (18)$$

and the product $I(u_1)I(v_1)$ becomes

$$I(u_1)I(v_1)=(1-i)(1-i)=-2i. \quad (19)$$

The substitution of (18) and (19) into (11) gives

$$P_\infty(f)\equiv\frac{B\mathscr{R}_{12}e^{-ik(R_1+R_2)}}{(R_1+R_2)}, \quad (20)$$

where we define the reference pressure $P_\infty(f)$. As expected, this is the image solution.[14]

B. Facet pressure reflection factor

We define a facet reflection factor as being the amplitude of the reflection from a facet relative to the reflection from an infinite plane interface. Let $G(f)$ be the ratio of the pressure reflected at a facet relative to the pressure reflected at an infinite plane. It is the ratio of (11) to (20):

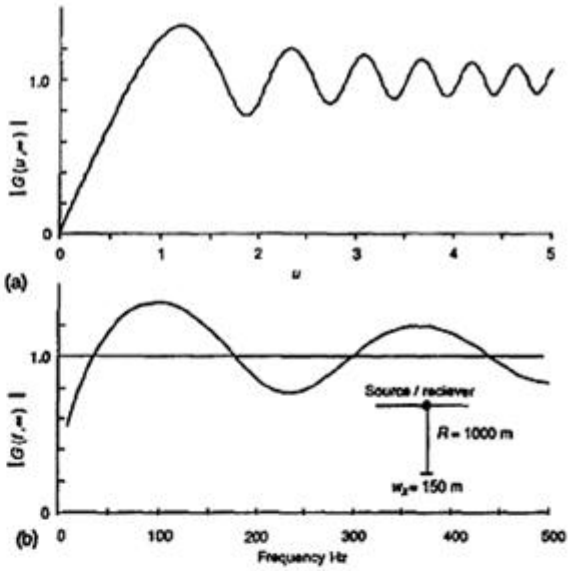

FIG. 3. Relative reflection amplitudes $G(u,\infty)$ and $G(f,\infty)$ as functions of facet width and frequency. The facet has infinite length in the y direction and finite width in the x direction. The harmonic source has frequency f. (a) Dependence on u. (b) Dependence on frequency for a finite width facet at the seafloor. The source and receiver are colocated as sketched in the inset. The relative reflection amplitude is normalized relative to the reflection from an infinite plane at the same range.

$$G(f)\equiv\frac{P(f)}{P_\infty(f)}=\frac{iI(u_1)I(v_1)}{2}. \quad (21)$$

By using the ratio of pressure reflections from the same materials, the reflection coefficients in (7) and (20) cancel.

The dependencies on the right side of (21) are on u_1 and v_1. Recall (21) and that $x_1=w_x/2$ and $y_1=w_y/2$. The subscripts on u_1 and v_1 in (21) are dropped, a range R^* is defined, and u and v are written as

$$u=w_x\cos\psi/(\lambda R^*)^{1/2}, \quad (22)$$

$$v=w_y/(\lambda R^*)^{1/2}, \quad (23)$$

$$R^*\equiv 2R_1R_2/(R_1+R_2).$$

The common monostatic condition, $R_1=R_2$, gives $R^*=R_1$. The facet reflection coefficient $G(f)$ becomes

$$G(u,v)\equiv iI(u)I(v)/2. \quad (24)$$

C. Semi-infinite facet examples

For the first example, we let w_y be infinite and calculate $G(u,v)$. Here, v becomes infinite. Using (18) to evaluate $I(v)$, $G(u,\infty)$ becomes

$$G(u,\infty)=(1+i)I(u)/2. \quad (25)$$

The absolute value of $|G(u,\infty)|$ is, using (14),

$$|G(u,\infty)|=\sqrt{2}[C^2(u)+S^2(u)]^{1/2}. \quad (26)$$

A numerical calculation for $G(u,\infty)$ is shown in Fig. 3(a). The dependence of $G(u,\infty)$ on u can be regarded as de-

pendencies on ψ, ranges R_1 and R_2, frequency or $\lambda=c/f$, and facet width w_x. The dependence of $G(f)$ on frequency for fixed w_x, ranges, and ψ is shown in Fig. 3(b).

The curves shown in Fig. 3 have slowly damped oscillations as u or f increases. These oscillations are related to the continuous wave or harmonic solution of the Helmholtz–Kirchhoff integral in the Fresnel approximation. Namely, *the contributions to the integral from each dS on S in Fig. 2 are present at all times.* Clay and Kinney (1988) discuss the implications of this requirement.[17] It affects the use of the Helmholtz–Kirchhoff integral in calculations of the reflections of incident transient pressures. Figure 3(b) shows the dependence of the relative reflection amplitude from a finite width plane facet at 1000-m depth. Geophysical examples that can be modeled by a set of plane facets are hard rock outcrops on continental shelves and basaltic lava flows at mid ocean ridge crests.

II. REFLECTION OF A TRANSIENT PRESSURE AT A FACET

A transient pressure reflection at a facet has a different and, as we will show, a simpler response than the reflection of a harmonic wave. The computation of the response is simpler in the frequency domain because the Fresnel function is in the frequency domain, i.e., u is a function of f as well as wedge width and geometry.

Adapting our notation of B for the source function, we let the source $b(t)$ have the spectrum $B(f)$ and transformation relation,

$$B(f)=\int_{-\infty}^{\infty} b(t)e^{-i2\pi ft}\,dt, \tag{27}$$

where $b(t)$ satisfies the usual conditions for the integral. The reflected pressure signal is the convolution of $B(f)$ and $P(f)$ in (11):

$$p(t)=\mathscr{R}_{12}\int_{-\infty}^{\infty} B(f)\frac{ie^{-ik(R_1+R_2)}}{2(R_1+R_2)}I(u)I(v)e^{i2\pi ft}\,df. \tag{28}$$

The integral of $p(t)^2$ is a common measure of the reflected signals. Parseval's theorem gives

$$\int_{-\infty}^{\infty} p(t)^2\,dt=\mathscr{R}_{12}^2\int_{-\infty}^{\infty}|B(f)|^2\frac{|I(u)I(v)|^2}{4(R_1+R_2)^2}\,df. \tag{29}$$

Recalling the pressure reflection from an infinite facet (20), the application of Parseval's theorem gives

$$\int_{-\infty}^{\infty} p_\infty(t)^2\,dt=\mathscr{R}_{12}^2\int_{-\infty}^{\infty}|B(f)|^2\frac{1}{(R_1+R_2)^2}\,df, \tag{30}$$

the ratio of (29) over (30) gives the integral square of the facet reflection response or *pressure-squared reflection factor,*

$$[g(u,v)]^2\equiv\frac{\int_{-\infty}^{\infty}p(t)^2\,dt}{\int_{-\infty}^{\infty}p_\infty(t)^2\,dt}. \tag{31}$$

We use the terminology *pressure squared* instead of intensity because intensity is pu, where u is the vector particle velocity and p is the scaler pressure. We measure and compute pressures. After application of Parseval's theorem, some of the geometrical terms cancel and the pressure-squared reflection factor (31) becomes

$$[g(u,v)]^2=\frac{\int_{-\infty}^{\infty}|B(f)|^2[|I(u)I(v)|^2/4]df}{\int_{-\infty}^{\infty}|B(f)|^2\,df}, \tag{32}$$

where $g(u,v)$ is a function of facet dimensions, geometry, and signal spectrum. In general, $g(u,v)$ does not reduce to a simpler expression.

A. Numerical evaluations for simple $b(t)$

A gated sine wave has the duration T_g and carrier frequency f_p. For simplicity, we let $b(t)$ be centered on $t=0$ as follows:

$$\begin{aligned} &b(t)=\sin(2\pi f_p t), \quad \text{for } -T_g/2<t<T_g/2,\\ &b(t)=0, \quad \text{otherwise.}\end{aligned} \tag{33}$$

Fourier transformation of $b(t)$ gives the spectrum

$$|B(f)|=\left|\frac{\sin[\pi(f-f_p)T_g]}{2\pi(f-f_p)}-\frac{\sin[\pi(f+f_p)T_g]}{2\pi(f+f_p)}\right|. \tag{34}$$

We also used the damped sine wave and, without changing notation, let

$$\begin{aligned} &b(t)=\exp(-t/T)\sin(2\pi f_p t), \quad \text{for } 0<t<\infty,\\ &b(t)=0, \quad \text{otherwise,}\end{aligned} \tag{35}$$

where T is the decay time. The complex spectrum of the damped sine wave is

$$B(f)=\frac{2\pi f_p}{(i2\pi f+1/T)^2+4\pi^2 f_p^2}. \tag{36}$$

All of these spectral functions have peaks near f_p. The reflection factor (32) was evaluated for the same geometry and facet dimensions as shown in Fig. 3, namely u,∞.

The reflection factor $g(u,\infty)$ for different types of signals are shown in Fig. 4. The dependence of u on w_x and the wavelength $\lambda_p=c/f_p$ is

$$u=w_x\cos\psi/(\lambda_p R^*)^{1/2}. \tag{37}$$

The reflection factor for a single cycle of a sine wave as a function of u is shown in Fig. 4(a). The response is nearly constant for $u>1.8$. Clay and Kinney (1988) used a lengthy time domain computation to get nearly the same result.[17] The reflection factor for two cycles of a sine wave is shown in Fig. 4(b) and the factor for a damped sine wave (35) is in Fig. 4(c). Increasing the duration of the signal causes the reflection factor to have more oscillations. Very large T_g in (33) and large T in (35) cause the reflection factor to approach the continuous wave signal example, Fig. 3(a).

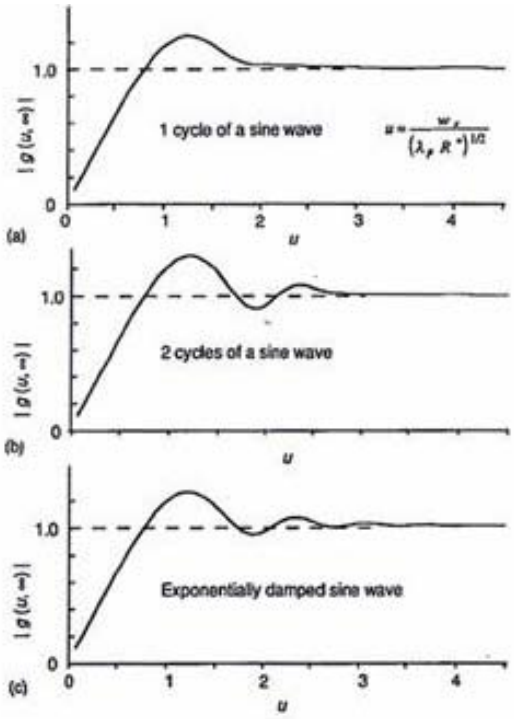

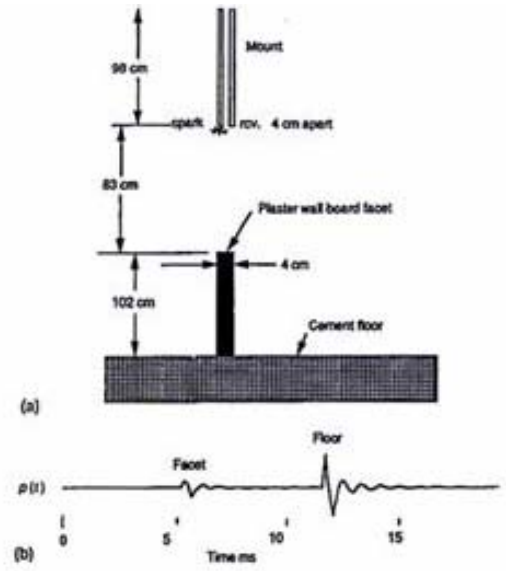

Fig.4 Fig.5

FIG.4.[on left] Relative reflection amplitudes of transient signals ?g(u,8)?

FIG. 5 [on right]. Laboratory experimental geometry and a pressure signal. (a) The experiments were made in air. The spark source and pressure receiver are nearly colocated. The facet is made of plaster wall board and the Boor is cement. The facet length 120 cm is effectively infinite. (b) Typical pressure signal. The direct arrival was suppressed. The reflection from the facet is called "facet" and the reflection from the Boor is labeled "floor." Diffraction arrivals are relatively small for this geometry.

III. EXPERIMENTS AND THEORY

Figure 5 shows a laboratory experiment and a typical signal.lg Relative to air, plaster wall board is very hard and dense and the reflection coefficient is nearly unity. These plaster materials damp vibrations and are good for laboratory acoustic experiments. The data were taken near vertical incidence and ?=0. The part of the signal labeled "Facet" was isolated from the rest of the signal to study the reflection from the 4-cm-width facet. The reference pressure or *p*8*(t)* was achieved by replacing the small facet by a large sheet of plaster sheet board at the same range. An example of an unfiltered *p*8*(t)* is shown in Fig. 6(a). We delayed digitization and recording of the signal until just before the signal arrived. The corresponding spectrum is labeled "source-system response" in Fig. 6(c). We digitally recorded *p*8*(t)* and then used FFT-filter-IFFT operations to calculate pressures for a set of signals having peak frequencies that range from 3 to 20 kHz. An example of filtered *p*8*(t)* for a peak frequency of 3 kHz is shown in Fig. 6(b) and its spectrum is shown in Fig. 6(c). The filtered domain signals were time shifted for display. The filtered *p*8*(t)* resembles a damped sine wave. Reflected sound pressures from the facets were processed the same way and filtered signals were computed for the pair, *p(t)* and *p*8*(t).* The wavelengths ?*p* that correspond to spectral peaks were computed for each pair of filtered signals. The ?p range, and facet widths were used to compute a and the experimental values of g exp(u, 8) shown in Fig. 7.

Theoretical calculations of g(u, 8), also shown in Fig. 7, used the damped sine wave signal (33) where the damping constant was

T=1/fP. (38)

The theoretical curve of g(u, oo) was computed as a function of *u,* i.e., *fP* using (32) and (36). The experimental values of g exp(u, 8) are a little larger than the theoretical curve between u=1 and 1.5.

IV. SOUND DEFLECTORS IN MUSIC HALLS

Sound deflectors are often placed over the stage in concert halls. As sketched in Fig. 8,

the deflector reflects some of the upward traveling sound waves from a performer on the stage into the seating area. The stage overhead and ceiling are not shown. Since deflectors are part of the stage, the designs can be rather decorative. Depending on the acoustical problems with the room, the sound deflectors may also be intended to reinforce specific frequency ranges. Sometimes designers use a "rule of thumb" that the deflectors scatter and reflect all waves that have ? less than the dimensions of the deflector. We believe that the finite facet theory gives an improved "rule of thumb."

The pressure facet reflection factor (21) gives the pressure reflected by a facet relative to the pressure reflected by an...

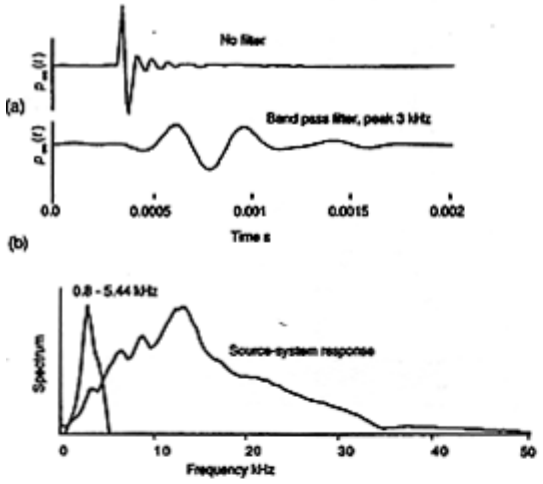

FIG. 6. Reflection from an infinite plane. All signal and spectral amplitudes are arbitrary. The time $t=0$ is chosen to be near the beginnings of the signals and the signals were time shifted for display. The travel times from the source to the reflecting interface and back to the receiver are suppressed. (a) The reflected signal from an "infinite" plane gives the system impulse response. (b) Bandpass-filtered signal for the bandpass 0.8–5.44 kHz filter. The filter operation was done digitally. (c) Spectra of the signals.

an infinite plane interface. The sketch in Fig. 8 shows the geometry of the performer, sound deflector, and listener. In auditoriums, acousticians often calculate the ratio of the reflected and scattered components to the direct sound from a performer. Here, we want the ratio of the reflected sound to the direct component. Accordingly, we modify $G(f)$ in (21) as follows:

$$G_d(f)\approx\frac{P(f)R_3}{P_\infty(f)(R_1+R_2)}\approx G(f)\,\frac{R_3}{(R_1+R_2)}, \quad (39)$$

where $G_d(f)$ is the facet pressure reflection factor relative to direct sound and R_3 is the direct range from the performer to the listener.

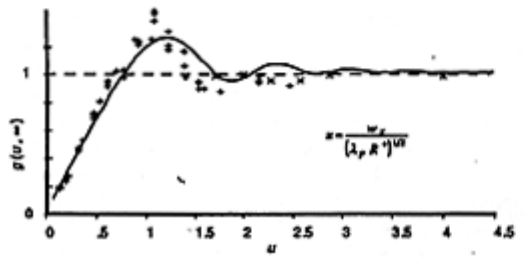

FIG. 7. Comparison of theory $g(u,\infty)$ and data, vertical incidence on finite width facets. The impulsive signals for the facet reflection, Fig. 5, were bandpass filtered as shown in Fig. 6. The peak frequencies were used to calculate the wavelength λ_p. The theoretical curve is the damped sine wave for $T=1/f_p$.

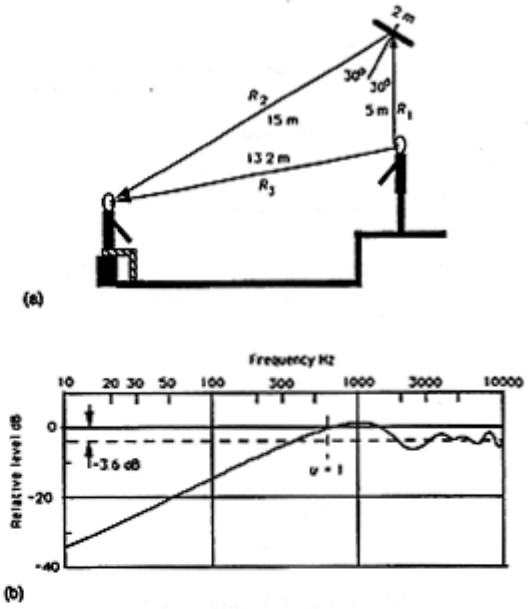

FIG. 8. Performance of a sound deflector over a performer. (a) Geometry. The distances are given on the sketch. (b) The sound level of the specularly reflected sound relative to the direct sound from the performer. The dashed line shows—3.6 dB that corresponds to the image sound level—the direct sound level.

The pressure reflection factor of a 2×2 m square deflector is also shown in Fig. 8. The response is in dB or $20\log_{10}|G_d(f)|$. Relative to the direct sound pressure level, the mean reflected sound-pressure level is $20\log_{10}[R_3/(R_1+R_2)]\approx-3.6$ dB in the image region above 200 Hz.

Figure 9 shows the reflection from a square facet, $u=v$. The Fraunhofer or incident plane-wave region requires that u be small and less than 0.5. The transition from Fraunhofer to Fresnel or incident spherical waves starts at u more than 0.5. The response oscillates about the image response of 1 at large u.

V. DISCUSSION AND CONCLUSIONS

Evaluations of the Helmholtz–Kirchhoff (H–K) integral in Fresnel approximation gives accurate amplitudes of the pressures that are specularly reflected at finite-dimensioned plane rigid facets. This theory is accurate for both continuous waves[1] and transient pressures. Explicit computations of diffraction components are not included in our evaluations of the H–K integral.

The literature also has "diffraction interpretations" of impulsive evaluations of the H–K integral, Trorey (1970)[19] and C-M, Sec. 10.2.[15] However, comparisons of these interpretations to the exact Biot–Tolstoy solution[8,9] and experiments show the Trorey solutions do not give correct diffracted components.[20] Clay and Kinney (1988) discuss the problem in detail.[17] Theoretical solutions need to consider spherical waves from point sources because

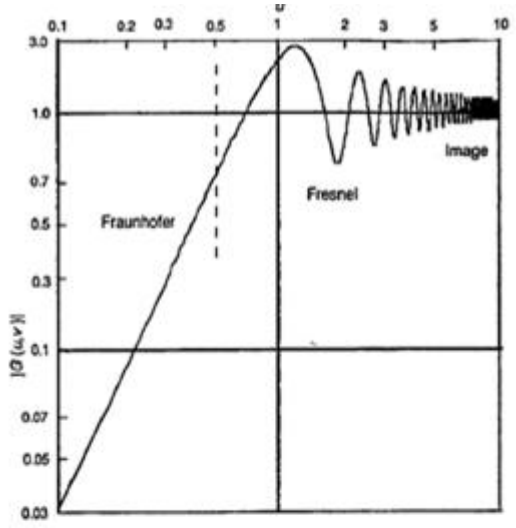

FIG. 9. Reflection from a square facet relative to an infinite plane The sound waves are vertically incident and $v=0$. In the Fraunhofer region, the dimensions of the square facet are less than the first Fresnel zone. For a harmonic wave, the Fresnel region is oscillatory and oscillates above and below the image limit of one.

incident plane-wave analysis is unlikely to give correct amplitudes for reflected components. Numerical studies show that the scattering of incident plane waves by periodic wedge assemblies is completely described by the diffractions from wedge crests and troughs and have no reflected components.[5] Clearly there is work to be done.

A "rule of thumb" is useful for architectural applications. Referring to Figs. 8 and 9, the reflected sound level $20 \log_{10}|G_d(f)|$ is greater than -6 dB relative to the mean level, for u and v greater than 0.5. Putting this condition in the definition of u (37), a minimum facet dimension for w_x is

$$w_x > (\lambda_p R^*)^{1/2}/2 \cos\psi. \tag{40}$$

The minimum facet dimension for w_y follows the same rule.

Incident plane-wave theory is often used in scattering problems. Again, we use Fig. 9 to give a plane-wave rule of thumb. The response $G(u,v)$ is nearly proportional to u for $u<0.5$. Incident plane waves can be used when the maximum dimensions of the object are less than the corresponding u and $v<0.5$, that is

$$\text{maximum dimensions} < (\lambda_p R^*)^{1/2}/2. \tag{41}$$

The plane-wave condition depends on the range and wavelength. The plane-wave condition also gives the Fraunhofer region. The transition from the Fraunhofer region mainly occurs between $0.5<u<1$. At $u>2$, the reflection amplitudes are approximately given by image reflections.

ACKNOWLEDGMENTS

This paper is taken from a tutorial that was written after Clay's conversations with John Preston and others at the ASW Research Center, La Spezia, Italy. Herman Medwin gave our paper a delightfully critical review. Our research was supported by many individuals and sources. Support came from the following: the Center for Polar Research and the Department of Geology and Geophysics of the University of Wisconsin; the Office of Naval Research, Mr. Robert Obrochta (N00014-84-K-0611) and Dr. Joseph Kravitz (N00014-86-K-0323); Naval Research Laboratory-Stennis Space Center, Mr. Richard Keiffer (N00014-88-K-6007) and Mr. Roger Meredith (N0001491-J-6004); and the Ocean University of Quing Dao.

1. W. G. Neubauer and L. R. Dragonette, "Monostatic reflection from a rigid rectangular plate," J. Acoust. Soc. Am. 41, 656-661 (1967).

2. I. Tolstoy, "Diffraction by a hard truncated wedge ans a strip," IEEE J. Ocean Eng. 14, 4-16 (1989).

3. I. Tolstoy, "Exact, explicit solutions for diffraction by hard sound barriers and seamounts," J. Acoust. Soc. Am. 85, 661-669 (1989).
4. W. A. Kinney, C. S. Clay, and G. A. Sandness, "Scattering from a corrugated surface: Helmholtz-Kirchhoff theory and the facet-ensemble method," J. Acoust. Soc. Am. 73, 183-194 (1983).
5. J. C. Novarini and H. Medwin, "Computer modeling resonant sound scattered from a periodic assemblage of wedges: Comparisons with theories of diffraction gratings;' J. Acoust. Soc. Am. 73, 183-194 (1983).
6. H. Medwin, "Shadowing by finite noise barriers," J. Acoust. Soc. Am. 72, 1005-1013 (1982).
7. H. Medwin, E. Childs, and G. M. Jebsen, "Impulse studies in double diffraction: A discrete Huygens interpretation," 1. Acoust. Soc. Am. 73, 183-194 (1983).
8. M. A. Biot and I. Tolstoy, "Formulation of wave propagation in infinite media by normal coordinates with an application to diffraction," J. Acoust. Soc. Am. 29, 381-391 (1957).
9. Tolstoy and C. S. Clay, *Ocean Acoustics.'* Theory *and Experiment in Underwater Sound 2nd Edition* (American Institute of Physics, Now York, 1987), Appendix 5 is Ref. 8.
10. S. Li and C. S. Clay, "Sound transmission experiments from an impulsive source near rigid wedges," J. Acoust. Sac. Am. 84, 2135-2143 (1988).
11. D. Chu, "Impulse response of a density contrast wedge using normal coordinates," Ph.D. thesis, University of Wisconsin-Madison (1989). Extends the exact Riot Tolstoy solutiona~9 to fluid wedges having finite density contrasts. Again the exact solution is the sum of a diffraction term and "image" reflections.
12. D. Chu, "Impulse response of density contrast wedge using normal coordinates," J. Acoust. Soc. Am. 86, 1883-1896 (1989).
13. D. Chu, "Enact solution for a density contrast shallow-water wedge using normal coordinates," J. Acoust. Soc. Am. 87, 2442-2450 (1990).
14. C. S. Clay, *Elementary Exploration Seismology* (Prentice Hall, Eng1ewood Cliffs, NJ, 1990), Chap. 14 and Appendix C1.2.
15. C.S. Clay and Herman Medwin, *Acoustical Oceanography* (Wiley, New York, 1977), Sees. 10.4 and 10.5 and Appendix AI0.5.
16. M. Abramowitz and I. A. Stegun (Eds.), *Nand6ook of Mathematical Functions,* Appl. Math. Ser. 55 (National Bureau of Standards, U.S. Government Printing Office, Washington, DC, 1965).
17. C. S. Clay and W. A. Kinney, "Numerical computations of time domain diffractions from wedges and reflections from facets," J. Acoust. Soc. Am. 83, 2126-2133 (1988).
18. S. Li and C. S. Clay, "Experimentation of time domain di9'raedons from wedges and reflections from facets" (in Chinese), Acta Acustica 17, 56-64 (1992). Contains comparisons of the reflections of transient pressures from finite dimensioned facets and the theory in Ref. I7. The agreement is good.
19. A. W. Trorey, "A simple theory for seismic diffractions," Geophysics 35 762-784 (1970). Gives an impulsive evalution of the Helmholtz - The Kirchhoff integral, also known as the Rabinowitz solution [M. Born agreement is good. and E. Wolf, *Principles of Optics* (Pergamon, Oxford, 1965), Sec. 8.9].
20. M. Jebsen and H. Medwin, "On the failure of the Kirchhoff assumptions in backscatter," J. Acoust. Soc. Am. 72, 1607-1611 (1982).

From : The Journal of the Acoustical Society of America 94(1993)October, No.4, Woodbury,